Interaction Notes

Note 602

4 July 2006

Double-Pulse Technique for Defending from Hostile Systems

D. V. Giri
Pro-Tech, 11-C Orchard Court, Alamo, CA 94507-1541

and

Tai Tsun Wu
Gordon McKay Laboratory, Harvard University, Cambridge, MA 02138

Abstract

In this paper, we have addressed a promising way of defending from a hostile system, using two electromagnetic pulses. The first pulse is a hyperband signal meant to interrogate the target system to determine its vulnerabilities in terms of the frequencies that can penetrate the system. The second pulse is then tailored to contain the electromagnetic energy in the appropriate frequency band in an attempt to disable the hostile system. The possibility of such a double-pulse technique has been raised by many and we have decided to look into this further. The emerging technology of hyperband systems with bandratios of ~ 100 facilitates and inspires us to further investigate this technique. In a representative example considered in this note, we find that a single equation can lead to both external and internal resonances of the target system.

The work reported here is the result of an I R & D project in Pro-Tech.

1. Introduction

A promising way to defend against a hostile system in air, on water or land (ex: an incoming missile, speed boat or a ground vehicle with hostile intention) is to send a powerful electromagnetic pulse to disable the electronic control system. It is the purpose of this paper to discuss one aspect of such a defense. In the case of a missile, an alternative possibility is to send up an anti-missile to intercept the incoming missile. We are of the opinion that this alternative has uncertainties and the electromagnetic solution could complement the defense.

In order to disable the electronics some of the energy of the electromagnetic pulse must penetrate to the interior of the missile. If the outer shell of the hostile system is not highly conductive, this penetration can be accomplished with relative ease. Even if the outer shell is metallic, there are unavoidable points of entry consisting of junctions of metallic surfaces, slits around moving surfaces, inadvertent apertures etc, where the electromagnetic pulse can penetrate. Points of Entry (PoEn) for electromagnetic energy can also serve as Points of Exit (PoEx).

Such penetration into the system is more easily accomplished at some frequencies of the electromagnetic pulse than other frequencies. Therefore, the disabling of electronics can be more easily carried out if the pulse can be tailored to contain most of its energy in these frequencies. From this point of view, the defense can be accomplished in two successive stages.

1) We first send a moderately powerful electromagnetic pulse. Over certain frequency ranges, this pulse contains significant energies. We analyze the return signal to determine the frequencies that may have penetrated the target system, which are likely to be the frequencies where the system is vulnerable. It is noted that coupling of certain frequencies into the system is necessary, but may not be sufficient to accomplish the necessary damage.
2) We send a second pulse to disable the electronics of the system. This second pulse is much more powerful than the first electromagnetic pulse and is tailored to contain as much energy as possible in the frequencies that coupled into the system.

This procedure of using two electromagnetic pulses has the following side benefit. It is conceivable that systems of the same type can be individualized so that their responses to electromagnetic pulses are different from each other. Such a discriminating program does not have any effect on the present procedure of using two pulses.

The double-pulse defense has been suggested in the past by researchers including the first author of this paper. A general intuitive response has ranged from “this technique is not practical” to “it can not give the interior resonances”. The implied pessimism and finality of the responses has motivated us to look into this problem, in some detail.

a) Airborne Target System

We have considered a canonical problem representative of the missile defense in this paper. We find that in an idealized case, it is possible to write a single equation that yields both ***exterior*** and ***interior*** resonances. We believe this is a new result opening the door for pursuing this problem.

b) Water or Land borne Target System

The two scenarios where this double pulse technique could apply are:

i) Defending ships from hostile speed boats and
ii) Portal defense against hostile and speeding automobiles.

Consider the case of ship defense employing a 3-tier perimeter defense zones. These three areas are typically centered on the ship to be defended. The outermost area or the green zone where recreational and other vessels are permitted is followed by an orange zone where certain defensive measures are triggered. If the unknown water vessels (ex; speed boats) enter the red zone they could be disabled or fired upon if needed. The first of the two-pulse method is applied in monitoring the vessels in the green zone. The second pulse is applied while the unknown vessel enters the red zone. Such a method has several advantages.

1) No EM shield is perfect and there are almost always points of entry (PoEn) for EM energy into any electronic system.

2) Points of entry can also be viewed as points of exit (PoEx) for EM energy.

3) Attempts to change the resonances or additional shielding of the speed boat engines will not work, since vulnerabilities are determined for the "as configured" system and not for a generic model.

4) Speedboats with the additional shielding are found by the first pulse and if they approach dangerously close they are targeted.

5) This technique is nonlethal, i.e., if a mistake is made, there is no serious consequence such as the loss of life.

6) The necessity of monitoring the water vessels in the outer green zone serves also the purpose of keeping sailors/soldiers alert on the watch-out duty, avoiding the associated sheer boredom issues. The first pulse monitoring is not busy work, but may be essential for the survival of the ship.

7) The second pulse is intended to disable the approaching speed boat at close range. The results of applying the second pulse are immediately obvious, while reserving the last resort option of firing upon the speed boat with hostile intentions.

Considerations described above, in the context of ship defense are also applicable for the case of portals where the passing automobiles are required to stop for inspection.

In the past, Ziolkowski et al., [1] have considered the problem of scattering from an open spherical shell having a circular aperture and enclosing a concentric dielectric sphere. They look for resonances in the radar cross section and indicate that for cavity backed apertures there is interior information contained in the exterior scattering data, which is encouraging. Apertures in

conducting screens [2], slotted cylinders [3], and spherical cavities [4 and 5] have been studied from a diffraction point of view. The effect of small perturbations in the surface of a metallic sphere on the exterior resonances has been studied by Varvatsis [6] using perturbation theory. The problem of Nuclear Electromagnetic Pulse (NEMP) excitation of cavities through small apertures is discussed by Chen and Baum [7]. They characterize the electrically small aperture by its electric and magnetic polarizabilities to determine the interior resonant modes of the cavity.

We are looking at a somewhat different aspect of the problem than what has been reported in the literature cited above, excepting [1]. In the modern context, studying the back scattered fields from a target system for varying incidence parameters (angle and polarization) is already proving to have important benefits in target identification. This has been possible because hyperband systems have come on the scene [8, 9] and the return signals have rich information about the target exterior and potentially on the target interior resonances. We can now illuminate target systems with impulse-like waveforms lasting 100 - 200 ps [9] with huge interrogatory capabilities.

2. The basic Idea

Consider a closed surface of perfect conductor as shown in Figure 1.

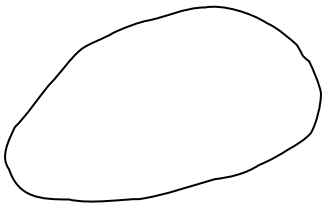

Figure 1. A perfect conducting surface enclosing a volume

There are exterior resonance frequencies $f_j^{(e)}$ and interior resonance frequencies $f_j^{(i)}$. Since there is no loss but there is radiation, we know:

- the $f_j^{(i)}$ are real
- the $f_j^{(e)}$ are complex with non-zero imaginary parts. (1)

If an electromagnetic spike is sent to scatter from such an object, we can determine from the return pulse:

- the $f_j^{(e)}$
- but not the $f_j^{(i)}$ (2)

On a fundamental level, we know the following:

(1) The interior resonance cannot "see infinity", meaning that the solution of the Maxwell equations is non-zero only in a finite region of the space. In particular, when there is no loss, the interior resonance frequencies are real.

(2) On the other hand, the exterior resonance can "see infinity", meaning that the corresponding solution of the Maxwell equation is non-zero in a region that extends to infinity. Even when there is no loss, the exterior resonance frequencies are complex.

We consider next the same closed surface of perfect conductor, but we make a hole on it:

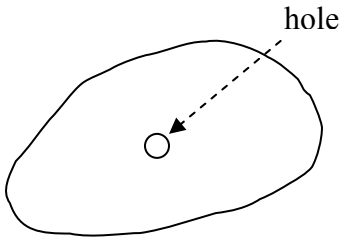

Figure 2. A perfect conducting surface (with a hole) enclosing a volume

Even when the remaining part of the closed surface is perfectly conducting, the interior and exterior are no longer isolated from each other. When the hole is small, the interior and exterior resonance frequencies are small perturbations from those without the hole. But the natures of the perturbations are qualitatively different.

(a) Since the external resonance frequencies are complex to begin with, the presence of the small hole causes a small shift in both the real part and the imaginary part.

(b) Although the interior resonance frequencies are real without the hole, the presence of the hole makes them complex. In the language of the (1) and (2) above, the interior resonance can now "see infinity" through the hole. Therefore all the interior resonance frequencies are also complex.

In other words, in the presence of the hole, there is no longer any qualitative difference between the interior resonance and the external resonance.

The basic idea is therefore this:

> *Because of the presence of joints and possibly other holes on the target system surface, the return signal from the missile due to an electromagnetic pulse contains information about the interior of the system.*

3. Simplest Example

In order to make the discussion concrete, it is always useful to have examples, especially those that demonstrate explicitly the main point of the idea.

We have been trying to formulate as simple an example as possible. It is believed that the following is the simplest non-trivial example.

A useful example should have the following properties. There is an interior region and an exterior region. These two regions should be coupled electromagnetically with a coupling that is described by one or more parameters. In the simplest case, the number of such parameters should be only one; let us call this parameter α, At some limiting value of this parameter α, these two regions become decoupled, there being interior resonance frequencies and external resonance frequencies. We want to study values of α that are close to, but not equal to, this limiting value.

Since we want to formulate the simplest example, we propose that the following should hold not only for the limiting value of α but also for <u>all</u> values of α.

(1) Since two-dimensional problems are easier to deal with than there-dimensional problems, this simplest example should be two-dimensional. This has the additional advantage that the vector nature of Maxwell's equations disappears and we are dealing with a scalar problem.

(2) Since we want the simplest example, we want maximum symmetry.

(3) Since the interior region must be of finite size, the maximum symmetry is achieved by rotational symmetry.

(4) This rotational symmetry should hold for <u>all</u> values of the parameter α.

(5) Since lossy problems are in general messier to deal with than those without energy dissipation, all energy dissipation should be avoided.

(6) Since we want to have an interior region and an exterior region, it is simplest to choose these two regions such that together they cover the entire two-dimensional space. Mathematically, what we are saying is that the union of the closure of the interior region and the closure of the exterior region is the entire two-dimensional space.

(7) This implies that the interior region and the exterior region communicate through a "wall" of zero thickness.

From these considerations, the following simplest example emerges, (as illustrated in Figure 3)

Maxwell's equations in free space are

$$\nabla \cdot \vec{D} = O \qquad \nabla \cdot \vec{B} = O$$
$$\nabla \times \vec{H} - \frac{\partial \vec{D}}{\partial t} = O \qquad \nabla \times \vec{E} + \frac{\partial \vec{B}}{\partial t} = O \tag{3}$$

For free space, $\vec{H} = \vec{B}/\mu_o$ and $\vec{D} = \varepsilon_o \vec{E}$, and we use $e^{-i\omega t}$ for sinusoidal time dependence.

For $k \neq 0$, $\nabla \cdot \vec{D} = 0$ and $\nabla \cdot \vec{B} = 0$ no longer contain any information. We therefore have

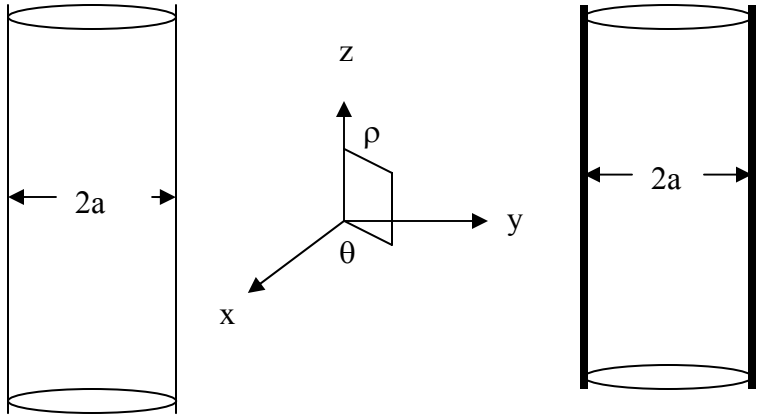

a) Infinite cylinder made of a perfect conductor

b) Same cylinder with a reactive (X_s) coating on the surface

Figure 3. Geometry of the problem

$$\nabla \times \vec{H} + i\omega \vec{D} = 0 \quad \text{or} \quad \nabla \times \vec{H} = -i\,\omega\varepsilon_0 E \tag{4}$$

$$\nabla \times \vec{E} - i\omega \vec{B} = 0 \quad \text{or} \quad \nabla \times \vec{E} = i\,\omega\mu_0 \vec{H} \tag{5}$$

For two-dimensional problems, it is convenient to use the cylindrical coordinates (ρ, θ, z) with both $\vec{E}$ and $\vec{B}$ independent of z, i.e., they are functions of ρ and θ only.

For two-dimensional problems, the components

$$E_z, B_\rho, B_\theta \quad \text{(Magnetic fields are transverse } \Rightarrow \text{ TM case)}$$
$$\text{and} \quad B_z, E_\rho, E_\theta \quad \text{(Electric fields are transverse } \Rightarrow \text{ TE case)} \tag{6}$$

are decoupled from each other. We can choose to work with either set of three components; for definiteness, let us choose the first set. We thus set

$$B_z = 0 \qquad E_\rho = 0 \quad and \quad E_\theta = 0 \tag{7}$$

The other components are then related by

$$\begin{aligned} \frac{1}{\rho}\left[\frac{\partial}{\partial\rho}(\rho\,\mathrm{B}_\theta) - \frac{\partial\,\mathrm{B}_\rho}{\partial\theta}\right] &= -\,i\omega\mu_o\varepsilon_o\mathrm{E}_z \\ \frac{1}{\rho}\frac{\partial E_z}{\partial\theta} &= i\omega\mathrm{B}_\rho \\ -\frac{\partial\mathrm{E}_z}{\partial\rho} &= i\,\omega\,\mathrm{B}_\theta \end{aligned} \tag{8}$$

These equations hold both for the interior region ρ < a and for the exterior region ρ > a.

It is natural to express both B_ρ *and* B_θ in terms of E_z. Let ϕ (ρ,θ) = E_z , then

$$\mathrm{B}_\rho = \frac{-i}{\omega}\frac{1}{\rho}\frac{\partial\phi}{\partial\theta} \qquad \text{and} \qquad \mathrm{B}_\theta = \frac{i}{\omega}\frac{\partial\phi}{\partial\rho} \tag{9}$$

This ϕ satisfies the wave equation (Helmholtz equation) $\left(\nabla^2 + k^2\right)\varphi(\rho,\theta) = 0$, or

$$\left[\frac{1}{\rho}\frac{\partial}{\partial\rho}\rho\frac{\partial}{\partial\rho} + \frac{1}{\rho^2}\frac{\partial^2}{\partial\theta^2} + k^2\right]\phi(\rho,\theta) = 0 \qquad (\rho \neq a) \tag{10}$$

Once again, this holds everywhere except for ρ = a.

We now turn to the important issue as to what we should put on the cylinder ρ = a, which is of zero thickness. There is very little choice. We must put there something with surface impedance. Moreover, the surface must be a reactance, in order to avoid energy dissipation, as we have discussed earlier under (5).

Let us skip the details at this point, because the result is precisely as expected, namely a delta function is added to equation (10):

$$\left[\frac{1}{\rho}\frac{\partial}{\partial\rho}\rho\frac{\partial}{\partial\rho} + \frac{1}{\rho^2}\frac{\partial^2}{\partial\theta^2} - \alpha\,\delta(\rho - a) + k^2\right]\phi(\rho,\theta) = 0 \qquad (\text{for } all\ \rho) \tag{11}$$

where α runs between 0 and + ∞ and has the units of inverse meter. Negative values of α are also allowed but do not seem to be useful to our understanding of the present problem of missile defense. One can show that this parameter α is given by

$$\alpha = \frac{\omega \mu_0}{X_s} \quad (m^{-1}) \quad \text{where } X_s \text{ is the surface reactance of the cylinder.}$$

When $\alpha \rightarrow +\infty$, then the interior region and the exterior region are no longer coupled. We are therefore primarily interested in large, positive value of α.

Because of rotational symmetry, which holds for all values of α, Fourier series expression can be used to reduce the partial differential equation to a set of uncoupled ordinary differential equations. They are

$$\left[\frac{1}{\rho}\frac{d}{d\rho}\rho\frac{d}{d\rho} - \frac{n^2}{\rho^2} - \alpha\,\delta(\rho - a) + k^2\right]\phi^{(n)}(\rho) = 0 \qquad \text{(for all } \rho\text{)} \tag{12}$$

where n is an integer (or half integer for that matter), and it may be taken to be a non-negative integer without loss of generality.

By the definition of the delta function, we have

$$\phi^{(n)'}(a+) - \phi^{(n)'}(a-) = \alpha\phi^{(n)}(a) \tag{13}$$

Of course $$\phi^{(n)}(a+) = \phi^{(n)}(a-) \overset{def}{=} \phi^{(n)}(a) \tag{14}$$

With the Sommerfeld radiation condition, we have, within irrelevant overall constants

$$\phi^{(n)}(\rho) = \begin{cases} \dfrac{J_n(k\rho)}{J_n(ka)} & \text{for} \quad \rho \le a \\ \dfrac{H_n^{(1)}(k\rho)}{H_n^{(1)}(ka)} & \text{for} \quad \rho \ge a \end{cases} \tag{15}$$

The boundary condition above then gives

$$k\frac{H_n^{(1)'}(ka)}{H_n^{(1)}(ka)} - k\frac{J_n'(ka)}{J_n(ka)} = \alpha \tag{16}$$

or $$k\,\frac{\dfrac{2i}{ka}}{J_n(ka)H_n^{(1)}(ka)} = \alpha$$

$$J_n(ka)H_n^{(1)}(ka) = \frac{2i}{\alpha a} \tag{17}$$

This is the desired answer. In the limit of $\alpha \to +\infty$, the above equation becomes

$$J_n(ka)\,H_n^{(1)}(ka)=0 \tag{18}$$

This factorizes into $J_n(ka)=0$ and $H_n^{(1)}(ka)=0$

$H_n^{(1)}(ka)=0$ gives the exterior resonance where k is complex

$J_n(ka)=0$ gives the interior resonance where k is real

This demonstrates explicitly that, in the limit $\alpha \to \infty$, the interior resonance and the exterior resonance are, as expected, separate and have nothing to do with each other.

On the other hand, for finite values of α, no matter how large, there is no such factorization, and the interior resonance and the exterior resonance are not separate. In particular, there is no fundamental difference between interior resonance and exterior resonance. They both "see infinity".

Let us study in more detail the case of large, positive value of α.

In this case, the right-hand side of equation (17) is small, and we expect to be able to apply perturbation theory.

Let k_0 be the solution of

$$J_n(k_0 a)=0 \tag{19}$$

Thus k_0 is real and positive. We expand the desired resonance frequency k in terms of k_0:

Thus

$$\begin{aligned} J_n(k_0 a) &= J_n\left(k_0\, a+\frac{k_1 a}{\alpha\, a}+\frac{k_2 a}{(\alpha\, a)^2}+\cdots\right) \\ &= J_n(k_0 a)+\left[\frac{k_1 a}{\alpha\, a}+\frac{k_2 a}{(\alpha\, a)^2}\right]J_n'(k_0 a)+\frac{1}{2}\left(\frac{k_1 a}{\alpha\, a}\right)^2 J_n''(k_0 a)+\cdots \\ &\approx \left[\frac{k_1 a}{\alpha\, a}+\frac{k_2 a}{(\alpha\, a)^2}\right]J_n'(k_0 a)+\frac{1}{2}\left(\frac{k_1 a}{\alpha\, a}\right)^2\left[-\frac{1}{k_0 a}\,J_n'(k_0 a)\right] \end{aligned} \tag{20}$$

Similarly, we have

$$\begin{aligned} \mathrm{Y}_n(k\,a) &= \mathrm{Y}_n\left(k_0\, a+\frac{k_1\, a}{\alpha\, a}+\cdots\right) \\ &\approx \mathrm{Y}_n(k_0\, a)+\frac{k_1 a}{\alpha\, a}\mathrm{Y}_n'(k_0\, a) \end{aligned} \tag{21}$$

and hence

$$\mathrm{H}_n^{(1)}(k\,a) \approx i\,\mathrm{Y}_n(k_0 a) + \frac{k_1\,a}{\alpha\,a}\mathrm{H}_n^{(1)'}(k_0\,a) \tag{22}$$

the substitution into equation (17) gives

$$\left\{\left[\frac{k_1\,a}{\alpha\,a} + \frac{k_2\,a}{(\alpha\,a)^2}\right] J_n'(k_0 a) + \frac{1}{2}\left(\frac{k_1\,a}{\alpha\,a}\right)^2 \frac{(-1)}{k_0\,a} J_n'(k_0 a)\right\}\left\{i\,\mathrm{Y}_n(k_0\,a) + \frac{k_1\,a}{\alpha\,a}\mathrm{H}_n^{(1)'}(k_0\,a)\right\}$$
$$= \frac{2i}{\alpha\,a} \tag{23}$$

or

$$\left[k_1\,a + \frac{k_2\,a}{\alpha\,a} - \frac{1}{2}\frac{(k_1\,a)^2}{k_0\,a\,\alpha\,a}\right] J_n'(k_0 a)\left[i\,\mathrm{Y}_n(k_0\,a) + \frac{k_1\,a}{\alpha\,a}\mathrm{H}_n^{(1)'}(k_0\,a)\right] = 2\,i \tag{24}$$

Therefore we get

$$k_1 = \frac{2}{a\,J_n'(k_0 a)\,\mathrm{Y}_n(k_0\,a)} \tag{25}$$

It is very surprising that k_1 is real. There must be a reason for this if this is true. Since $\mathrm{H}_n^{(1)'}(k\,a)$ is complex, there is no way for k_2 to be real.

4. Numerical Solution of Equation (17)

In this section we determine the zeros of equation (17) which is reproduced below by denoting z = x + i y = complex (ka) and A = $\alpha\,a$ with A being a real number.

$$J_n(z)\;\; H_n^{(1)}(z) = \frac{2\,i}{A} \tag{26}$$

We have numerically solved the above equation (26) for the cases of n = 0, 1, 2 and 3 and for $1 \le A \le 100$. We do know what happens for A = infinity when the above equation factorizes and the problem becomes that of finding the zeros of Bessel and Hankel functions. We are not particularly interested in the case of A = 0. In the case of A = 0, there is no wall and the problem becomes trivial.

Before we present the roots of equation (26), the Hankel function is calculated in its principal Riemann sheet ($-\pi < \arg\, z < \pi$) for n = 0, 1, 2 and 3. The Hankel-function magnitudes are presented in Figures 4 and 5. Figure 4 is for the cases of n = 0 and 1, while Figure 5 is for the cases of n = 2 and 3.

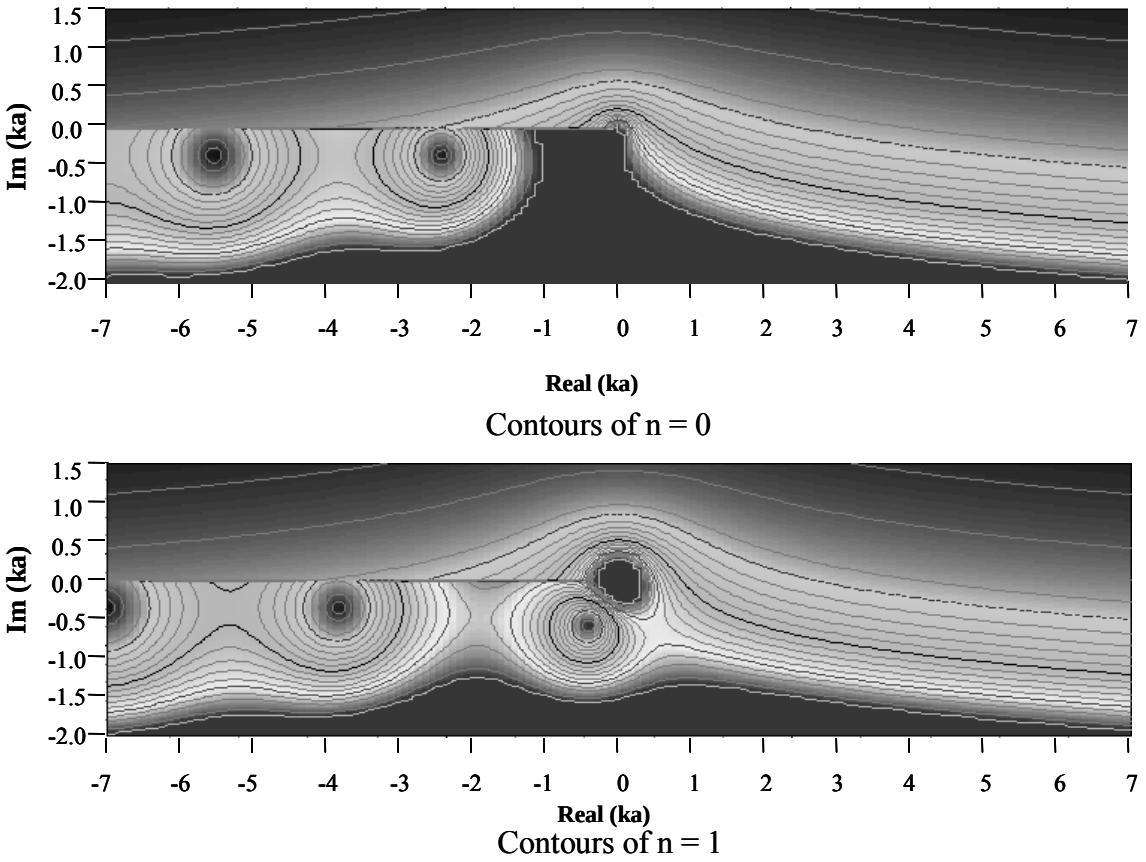

Figure 4. Contours of Hankel functions of the first kind $H_n^{(1)}(z = \text{complex ka})$ for the cases of n = 0 and 1, showing the zeros and the branch point at the origin and the branch cut along the negative real axis

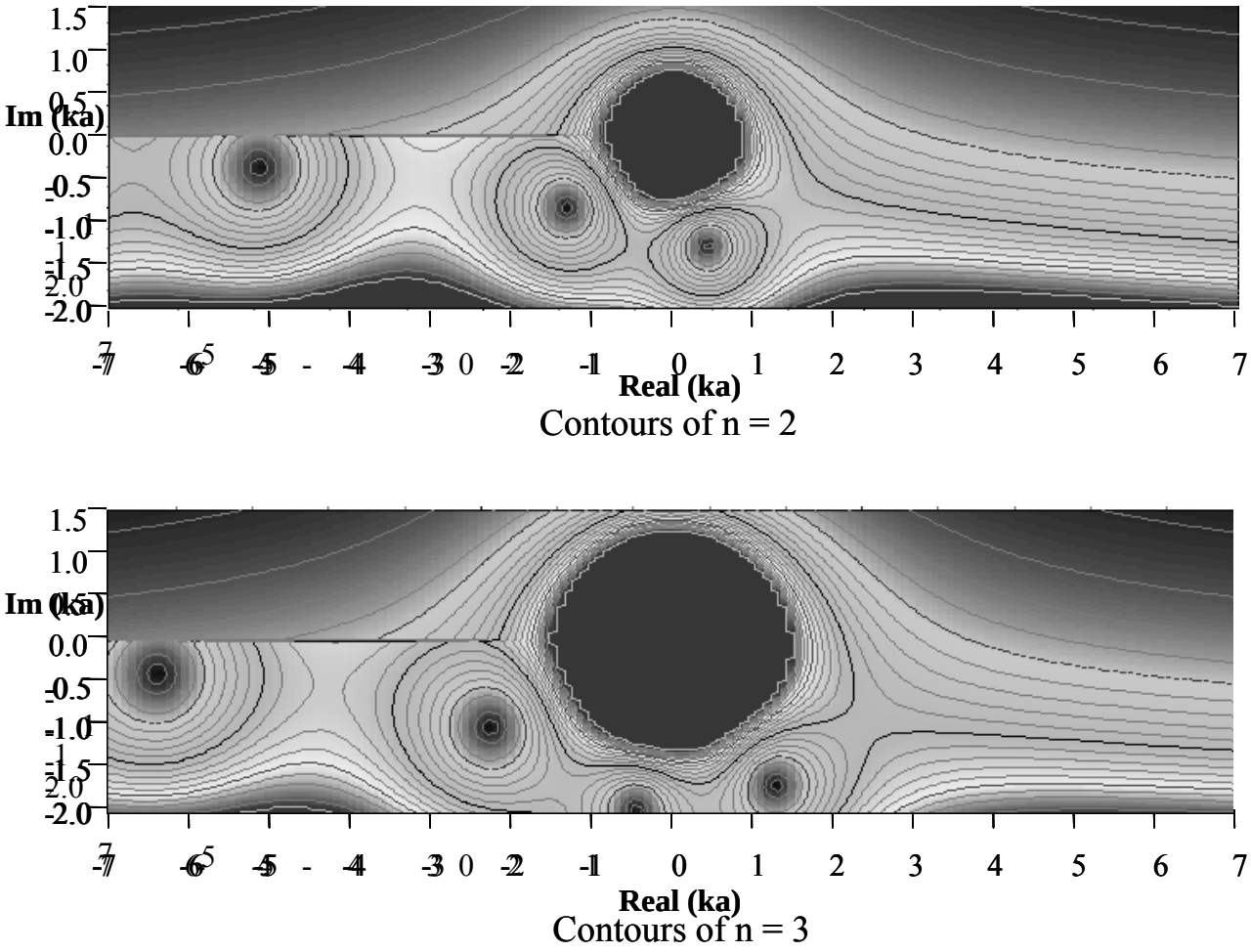

Figure 5. Contours of Hankel functions of the first kind $H_n^{(1)}(z = \text{complex ka})$ **for the cases of n = 2 and 3, showing the zeros and the branch point at the origin and the branch point along the negative real axis**

The location of the zeros in the complex z = ka plane agrees well with documented values in the literature for the Hankel functions [10, 11].

The trajectories of the roots of equation (26) and their numerical values are shown in Figures 6,7,8 and 9 and Tables 1, 2 3 and 4, for n = 0, 1, 2 and 3.

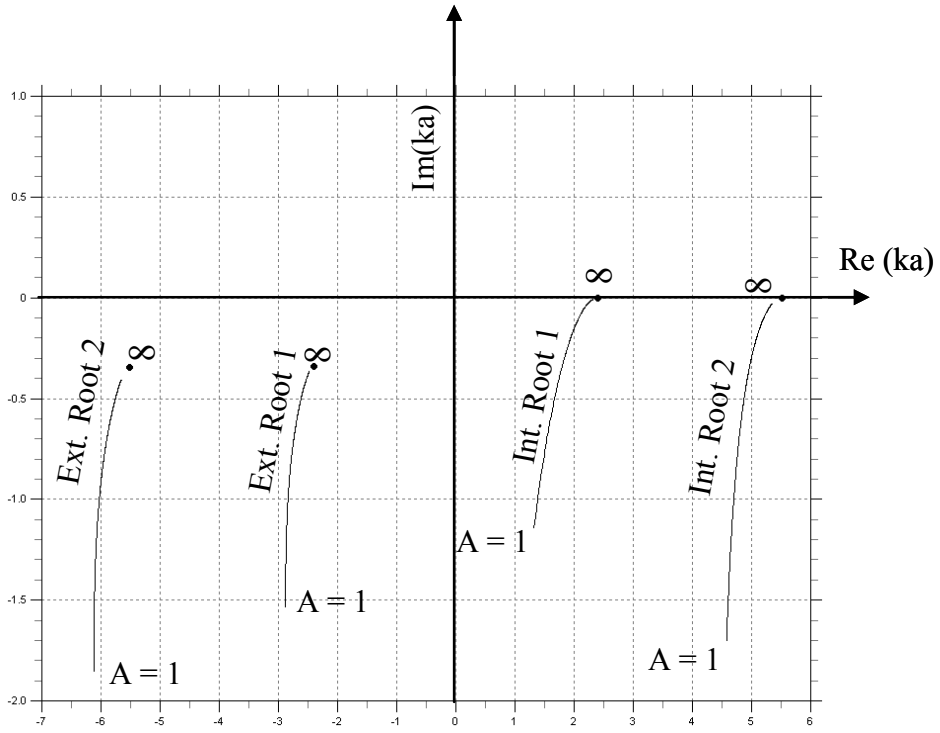

Figure 6. Four roots of Equation (26) in the lower half of complex (ka) = z = (x + iy) plane for the case of n = 0

	Interior	Root 1	Interior	Root 2	Exterior	Root 1	Exterior	Root 2
A	Re(ka)	Im(ka)	Re(ka)	Im(ka)	Re(ka)	Im(ka)	Re(ka)	Im(ka)
1	1.32E+00	-1.14E+00	4.58E+00	-1.70E+00	-2.88E+00	-1.53E+00	-6.12E+00	-1.85E+00
2	1.49E+00	-7.84E-01	4.63E+00	-1.35E+00	-2.87E+00	-1.20E+00	-6.11E+00	-1.51E+00
4	1.68E+00	-4.88E-01	4.70E+00	-9.98E-01	-2.82E+00	-9.10E-01	-6.07E+00	-1.19E+00
6	1.79E+00	-3.46E-01	4.75E+00	-8.01E-01	-2.77E+00	-7.69E-01	-6.03E+00	-1.01E+00
8	1.87E+00	-2.61E-01	4.80E+00	-6.67E-01	-2.73E+00	-6.84E-01	-6.00E+00	-9.02E-01
10	1.93E+00	-2.05E-01	4.84E+00	-5.67E-01	-2.70E+00	-6.28E-01	-5.96E+00	-8.23E-01
20	2.11E+00	-8.35E-02	5.00E+00	-2.98E-01	-2.61E+00	-4.96E-01	-5.86E+00	-6.28E-01
30	2.19E+00	-4.48E-02	5.10E+00	-1.82E-01	-2.57E+00	-4.44E-01	-5.80E+00	-5.46E-01
40	2.24E+00	-2.77E-02	5.17E+00	-1.21E-01	-2.54E+00	-4.16E-01	-5.76E+00	-4.99E-01
50	2.27E+00	-1.88E-02	5.23E+00	-8.62E-02	-2.52E+00	-3.99E-01	-5.73E+00	-4.69E-01
60	2.29E+00	-1.36E-02	5.27E+00	-6.41E-02	-2.51E+00	-3.87E-01	-5.71E+00	-4.48E-01
70	2.30E+00	-1.02E-02	5.30E+00	-4.93E-02	-2.50E+00	-3.79E-01	-5.69E+00	-4.32E-01
80	2.31E+00	-7.99E-03	5.32E+00	-3.91E-02	-2.49E+00	-3.73E-01	-5.67E+00	-4.20E-01
90	2.32E+00	-6.41E-03	5.34E+00	-3.17E-02	-2.48E+00	-3.68E-01	-5.66E+00	-4.11E-01
100	2.33E+00	-5.25E-03	5.36E+00	-2.62E-02	-2.47E+00	-3.65E-01	-5.65E+00	-4.03E-01
infinity	2.4048	0	5.5201	0	-2.404	-0.341	-5.52	-0.345

Table 1. Numerical values of the roots plotted in Figure 6 for the case of n = 0; (the values of the roots for the case A = infinity agree well with what is available in the literature)

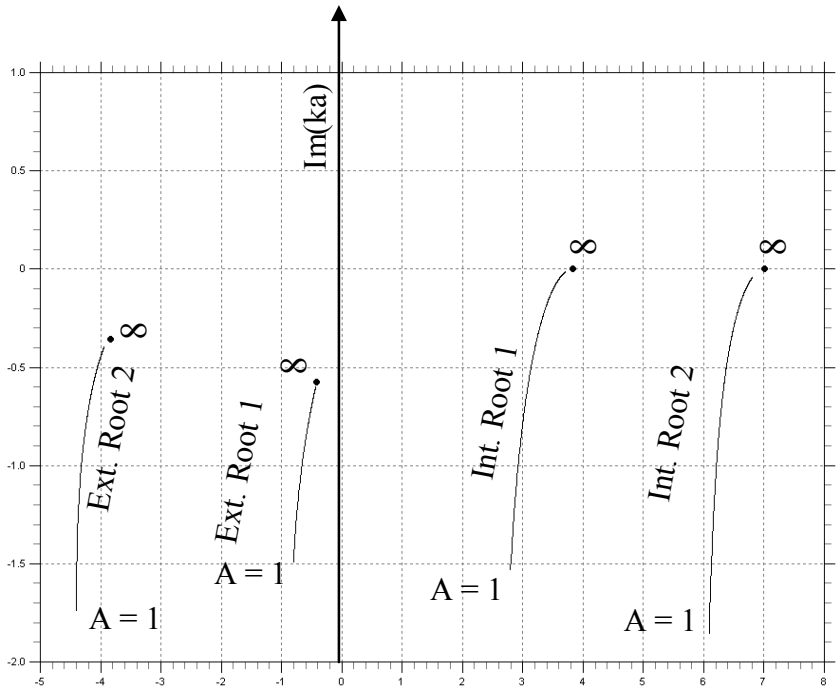

Figure 7. Four roots of Equation (26) in the lower half of complex (ka) = z = (x + iy) plane for the case of n = 1.

	Interior	Root 1	Interior	Root 2	Exterior	Root 1	Exterior	Root 2
A	Re(ka)	Im(ka)	Re(ka)	Im(ka)	Re(ka)	Im(ka)	Re(ka)	Im(ka)
1	2.80E+00	-1.53E+00	6.09E+00	-1.85E+00	-8.01E-01	-1.49E+00	-4.40E+00	-1.74E+00
2	2.88E+00	-1.15E+00	6.13E+00	-1.50E+00	-7.25E-01	-1.17E+00	-4.39E+00	-1.40E+00
4	3.00E+00	-7.85E-01	6.18E+00	-1.14E+00	-6.31E-01	-9.31E-01	-4.34E+00	-1.08E+00
6	3.09E+00	-5.93E-01	6.23E+00	-9.41E-01	-5.80E-01	-8.30E-01	-4.29E+00	-9.12E-01
8	3.16E+00	-4.69E-01	6.26E+00	-8.01E-01	-5.49E-01	-7.74E-01	-4.25E+00	-8.11E-01
10	3.21E+00	-3.82E-01	6.30E+00	-6.94E-01	-5.27E-01	-7.39E-01	-4.22E+00	-7.41E-01
20	3.40E+00	-1.74E-01	6.43E+00	-3.94E-01	-4.79E-01	-6.62E-01	-4.11E+00	-5.74E-01
30	3.51E+00	-9.88E-02	6.53E+00	-2.54E-01	-4.60E-01	-6.35E-01	-4.06E+00	-5.06E-01
40	3.57E+00	-6.30E-02	6.61E+00	-1.75E-01	-4.50E-01	-6.21E-01	-4.02E+00	-4.68E-01
50	3.62E+00	-4.35E-02	6.66E+00	-1.27E-01	-4.45E-01	-6.13E-01	-4.00E+00	-4.44E-01
60	3.65E+00	-3.18E-02	6.71E+00	-9.63E-02	-4.40E-01	-6.07E-01	-3.98E+00	-4.28E-01
70	3.67E+00	-2.42E-02	6.74E+00	-7.50E-02	-4.38E-01	-6.03E-01	-3.96E+00	-4.16E-01
80	3.69E+00	-1.90E-02	6.77E+00	-6.00E-02	-4.35E-01	-6.00E-01	-3.95E+00	-4.06E-01
90	3.71E+00	-1.53E-02	6.79E+00	-4.90E-02	-4.34E-01	-5.97E-01	-3.94E+00	-3.99E-01
100	3.72E+00	-1.26E-02	6.81E+00	-4.07E-02	-4.32E-01	-5.95E-01	-3.93E+00	-3.94E-01
Infinity	3.8317	0	7.0156	0	-0.419	-0.577	-3.832	-0.355

Table 2. Numerical values of the roots plotted in Figure 7 for the case of n = 1; (the values of the roots for the case A = infinity agree well with what is available in the literature)

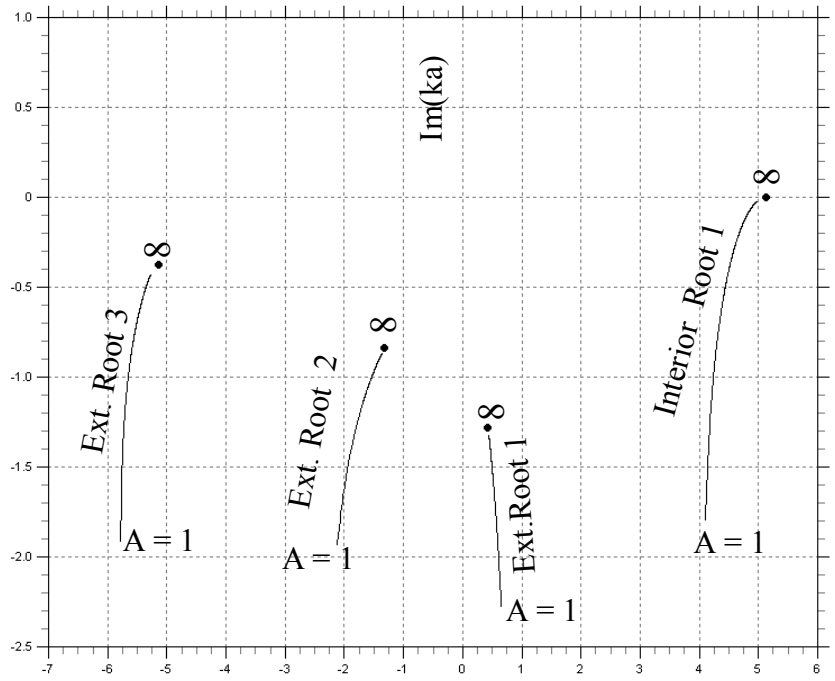

Figure 8. Four roots of Equation (26) in the lower half of complex (ka) = z = (x + iy) plane for the case of n = 2.

	Exterior	Root 1	Interior	Root 1	Exterior	Root 2	Exterior	Root 3
A	Re(ka)	Im(ka)	Re(ka)	Im(ka)	Re(ka)	Im(ka)	Re(ka)	Im(ka)
1	6.50E-01	-2.27E+00	4.11E+00	-1.79E+00	-2.12E+00	-1.93E+00	-5.78E+00	-1.91E+00
2	6.09E-01	-2.01E+00	4.16E+00	-1.39E+00	-1.98E+00	-1.59E+00	-5.76E+00	-1.55E+00
4	5.65E-01	-1.79E+00	4.24E+00	-9.96E-01	-1.82E+00	-1.30E+00	-5.71E+00	-1.21E+00
6	5.41E-01	-1.67E+00	4.31E+00	-7.77E-01	-1.72E+00	-1.18E+00	-5.67E+00	-1.04E+00
8	5.24E-01	-1.61E+00	4.37E+00	-6.32E-01	-1.65E+00	-1.10E+00	-5.62E+00	-9.21E-01
10	5.12E-01	-1.56E+00	4.42E+00	-5.27E-01	-1.60E+00	-1.06E+00	-5.59E+00	-8.41E-01
20	4.80E-01	-1.44E+00	4.61E+00	-2.60E-01	-1.48E+00	-9.55E-01	-5.47E+00	-6.45E-01
30	4.66E-01	-1.40E+00	4.73E+00	-1.54E-01	-1.44E+00	-9.18E-01	-5.41E+00	-5.64E-01
40	4.58E-01	-1.37E+00	4.80E+00	-1.01E-01	-1.41E+00	-8.98E-01	-5.37E+00	-5.19E-01
50	4.53E-01	-1.35E+00	4.86E+00	-7.07E-02	-1.39E+00	-8.86E-01	-5.34E+00	-4.89E-01
60	4.50E-01	-1.34E+00	4.90E+00	-5.22E-02	-1.38E+00	-8.78E-01	-5.32E+00	-4.68E-01
70	4.47E-01	-1.34E+00	4.93E+00	-4.00E-02	-1.37E+00	-8.72E-01	-5.30E+00	-4.53E-01
80	4.45E-01	-1.33E+00	4.95E+00	-3.16E-02	-1.37E+00	-8.68E-01	-5.29E+00	-4.42E-01
90	4.43E-01	-1.32E+00	4.97E+00	-2.56E-02	-1.36E+00	-8.65E-01	-5.28E+00	-4.32E-01
100	4.42E-01	-1.32E+00	4.98E+00	-2.11E-02	-1.36E+00	-8.62E-01	-5.27E+00	-4.25E-01
Infinity	0.429	-1.281	5.1356	0	-1.317	-0.836	-5.138	-0.372

Table 3. Numerical values of the roots plotted in Figure 8 for the case of n = 2; (the values of the roots for the case A = infinity agree well with what is available in the literature)

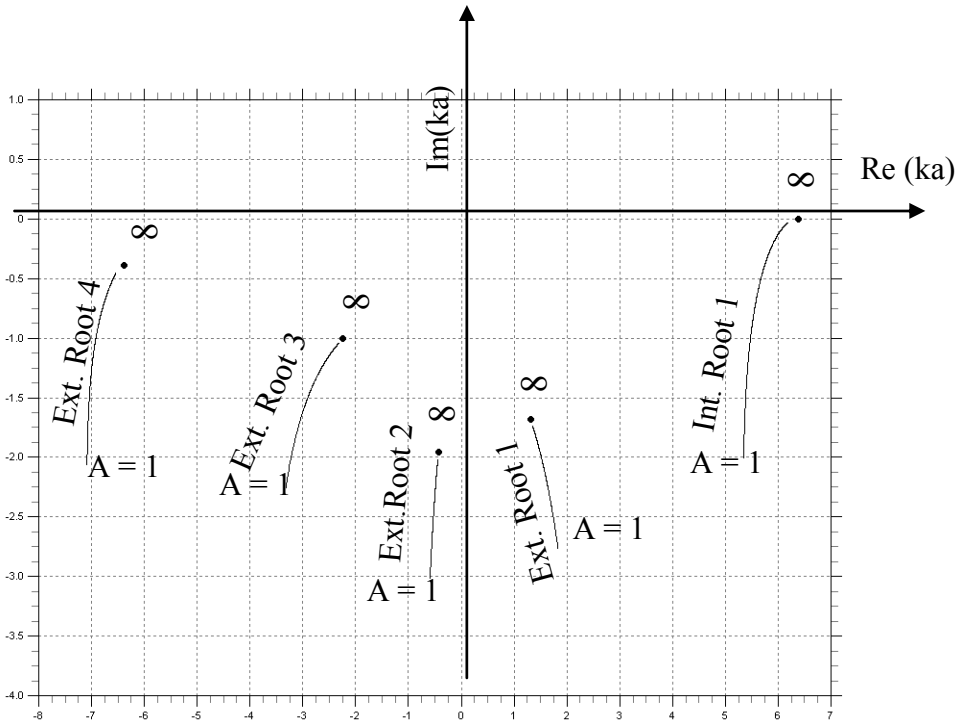

Figure 9. Four roots of Equation (26) in the lower half of complex (ka) = z = (x + iy) plane for the case of n = 3.

	Exterior	Root 1	Interior	Root 1	Exterior	Root 2	Exterior	Root 3	Exterior	Root 4
A	Re(ka)	Im(ka)	Re(ka)	Im(ka)	Re(ka)	Im(ka)	Re(ka)	Im(ka)	Re(ka)	Im(ka)
1	1.83E+00	-2.76E+00	5.35E+00	-2.00E+00	-5.92E-01	-3.01E+00	-3.32E+00	-2.25E+00	-7.09E+00	-2.06E+00
2	1.74E+00	-2.50E+00	5.37E+00	-1.58E+00	-5.64E-01	-2.77E+00	-3.16E+00	-1.88E+00	-7.06E+00	-1.69E+00
4	1.65E+00	-2.26E+00	5.44E+00	-1.17E+00	-5.35E-01	-2.55E+00	-2.96E+00	-1.57E+00	-7.01E+00	-1.34E+00
6	1.59E+00	-2.14E+00	5.49E+00	-9.30E-01	-5.19E-01	-2.44E+00	-2.83E+00	-1.42E+00	-6.97E+00	-1.14E+00
8	1.55E+00	-2.07E+00	5.55E+00	-7.70E-01	-5.08E-01	-2.36E+00	-2.74E+00	-1.33E+00	-6.93E+00	-1.02E+00
10	1.52E+00	-2.02E+00	5.60E+00	-6.52E-01	-4.99E-01	-2.31E+00	-2.68E+00	-1.27E+00	-6.89E+00	-9.30E-01
20	1.45E+00	-1.88E+00	5.78E+00	-3.40E-01	-4.76E-01	-2.18E+00	-2.51E+00	-1.15E+00	-6.77E+00	-7.10E-01
30	1.41E+00	-1.83E+00	5.90E+00	-2.08E-01	-4.65E-01	-2.12E+00	-2.43E+00	-1.11E+00	-6.70E+00	-6.17E-01
40	1.39E+00	-1.80E+00	5.98E+00	-1.39E-01	-4.58E-01	-2.09E+00	-2.39E+00	-1.08E+00	-6.65E+00	-5.65E-01
50	1.38E+00	-1.78E+00	6.04E+00	-9.94E-02	-4.54E-01	-2.06E+00	-2.37E+00	-1.07E+00	-6.62E+00	-5.31E-01
60	1.37E+00	-1.76E+00	6.09E+00	-7.41E-02	-4.51E-01	-2.05E+00	-2.35E+00	-1.06E+00	-6.60E+00	-5.07E-01
70	1.36E+00	-1.75E+00	6.12E+00	-5.72E-02	-4.48E-01	-2.04E+00	-2.33E+00	-1.05E+00	-6.58E+00	-4.89E-01
80	1.35E+00	-1.74E+00	6.15E+00	-4.55E-02	-4.47E-01	-2.03E+00	-2.32E+00	-1.05E+00	-6.56E+00	-4.75E-01
90	1.35E+00	-1.74E+00	6.17E+00	-3.69E-02	-4.45E-01	-2.02E+00	-2.32E+00	-1.04E+00	-6.55E+00	-4.64E-01
100	1.35E+00	-1.73E+00	6.19E+00	-3.06E-02	-4.44E-01	-2.02E+00	-2.31E+00	-1.04E+00	-6.54E+00	-4.55E-01
Infinity	1.308	-1.682	6.3802	0	-0.432	-1.959	-2.243	-1.007	-6.383	-0.389

Table 4. Numerical values of the roots plotted in Figure 9 for the case of n = 3; (the values of the roots for the case A = infinity agree well with what is available in the literature)

5. Summarizing Remarks

From this simple example, it is evident that when points of entry for EM energy exist, the interior and exterior resonances of the target system are qualitatively the same. In other words, they both have complex resonances in the complex frequency plane.

In the limit of the parameter A (characterizing the coupling of two regions) tending to infinity which represents the case of uncoupled interior and exterior resonances, the interior resonances are given by real values of (ka), and the exterior resonances are complex. In the context of missile defense, the realistic values of the parameter A are likely to be large but not infinity (no EM shield is perfect). In this case, the interior resonances become complex, but still in the proximity of the positive real axis in the fourth quadrant of the complex k plane. It is noted that the coupling coefficients of such resonances are necessarily small [12] and approaching zero for resonances on the positive real axis of the complex k plane. This is a signal/noise issue in processing the return signal resulting from illumination of the target system with a hyperband signal, or the first of the double pulses.

In our two pulse procedure, the return signal from the first Hyperband illumination is analyzed for the resonance mix. We then look for identifying the interior resonances which are likely to be in the fourth quadrant of the complex k plane with small imaginary parts. In the simple problem considered here, there are no difficulties in separating the interior and exterior resonances. This delineation of interior and exterior resonances is likely to hold for the realistic missile return signals. Identification of the interior resonances leads to the more important second-pulse excitation (narrow or moderate band signals) with its energy concentrated in the interior resonance bands.

Acknowledgment

We are grateful to Mr. Terry Brown who assisted with the numerical calculations. We also thank Dr. Carl Baum and Dr. Fred Tesche who offered useful comments.

References

1. R. W. Ziolkowski, D. P. Marsland, L. F. Libelo, Jr., and G. E. Pisane, "Scattering from an Open Spherical Shell Having a Circular Aperture and Enclosing a Concentric Dielectric Sphere," *IEEE Transactions on Antennas and Propagation*, Volume 36, Number 7, July 1988, pp 985-999.
2. L. F. Libelo and J. Bombardt, "Scattering of Electromagnetic Radiation by Apertures: Normal Incidence on the Slotted Plane, *Interaction Note* 106, 2 April 1970.
3. J. N. Bombardt and L. F. Libelo, "Scattering of Electromagnetic Radiation by Apertures: An Alternative Integral Equation with Analytic Kernels for the Slotted Cylinder Problem," I*nteraction Note 108*, March 1972.
4. T. B. A. Senior and G. A. Desjardins, "Field Penetration into a Spherical Cavity," *Interaction Note 142*, August 1973.
5. S. Chang and T. B. A. Senior, "Scattering by a Spherical Shell with a Circular Aperture," *Interaction Note 141*, April 1969.

6. A. D. Varvatsis, "EEM and SEM Parameter Variation due to Surface Perturbations of a Metallic Cylinder," *Interaction Note 357*, March 1979.
7. K. C. Chen and C. E. Baum, "On EMP Excitations of Cavities with Small Openings," *Interaction Note 170*, 2 January 1970.
8. D. V. Giri and F. M. Tesche, "Classification of Intentional Electromagnetic Environments (IEME)," *IEEE Transactions on Electromagnetic Compatibility, Special Issue on High-Power Electromagnetics (HPEM) and Intentional Electromagnetic Interference (IEMI),*" Volume 46, Number 3, August 2004, pp 322-328.
9. C. E. Baum, W. L. Baker, W. D. Prather, J. M. Lehr, J. P. O'Loughlin, D. V. Giri, I. D. Smith, R. Altes, J. Fockler, D. McLemore, M. D. Abdalla and M. C. Skipper, "JOLT: A Highly Directive, Very Intensive, Impulse-Like Radiator," *Proceedings of the IEEE Special Issue on Pulsed Power Technology & Applications*, Volume 92, Number 7, July 2004, pp 1096-1109.
10. **Handbook of Mathematical Functions**, Edited by M. Abramowitz and I. A. Stegun, Dover Publications Inc., New York, 1965, Figure 9.4, page 359.
11. A. Cruz, J. Esparaza, and J. Sesma, "Zeros of Hankel Function of Real Order out of the Principal Reimann Sheet," *Journal of Computational and Applied Mathematics*, Volume 37 1991, pp 89-99.
12. C. E. Baum, "On the Singularity Expansion Method for the Solution of Electromagnetic Interaction problems," *Interaction Note 88*, 11 December 1971.